Liquid-liquid interfaces enable tunable cell confinement to recapitulate surrounding tissue deformations during neutrophil interstitial migration *in vivo*

Jonathan H. Schrope[1,2,3,4], Adam Horn[2], Mehtab Farooqui[3,6], Kaitlyn Lazorchak[2,4], Jiayi Li[1], Clyde Tinnen[3], Jack J Stevens[1], David Bennin[5], Tanner Robertson[2], Terry Juang[1,3], Chao Li[5,ζ,*], Anna Huttenlocher[2,6,ζ,*], David J Beebe[1,3,5,ζ,*]

[1]Department of Biomedical Engineering, University of Wisconsin-Madison, Madison, WI, USA

[2]Department of Medical Microbiology and Immunology, University of Wisconsin-Madison, Madison, WI, USA

[3]Department of Pathology and Laboratory Medicine, University of Wisconsin-Madison, Madison, WI, USA

[4]Medical Scientist Training Program, University of Wisconsin-Madison, Madison, WI, USA

[5]Carbone Cancer Center, University of Wisconsin-Madison, Madison, WI, USA

[6]Department of Pediatrics, University of Wisconsin-Madison, Madison, WI, USA

ζ These authors contributed equally

* Co-corresponding authors

ABSTRACT

Cell migration is regulated by an interplay between both chemical and mechanical cues. Immune cells navigate through interstitial spaces and generate forces to deform surrounding cells, which in turn exert opposing pressures that regulate cell morphology and motility mechanisms. Current *in vitro* systems to study confined cell migration largely utilize rigid materials orders of magnitude stiffer than surrounding cells, limiting insights into how these local physical interactions regulate interstitial cell motility. Here, we first characterize mechanical interactions between neutrophils and surrounding cells in larval zebrafish and subsequently engineer *in vitro* migration channels bound by a deformable liquid-liquid interface that responds to cell generated pressures yielding a gradient of confinement across the length of a single cell. Tuning confining pressure gradients replicates mechanical interactions with surrounding cells during interstitial migration *in vivo*. We find that neutrophils favor a bleb-based mechanism of force generation to deform a barrier applying cell-scale confining forces. This work introduces a biomimetic material interface that enables new avenues of exploring the influence of mechanical forces on cell migration.

INTRODUCTION

Precise regulation of immune cell migration to sites of infection, malignancy, and injury is required for successful mounting and resolution of the immune response[1–4]. This process is tightly regulated *in vivo* by a combination of chemical gradients and local mechanical cues[3,4]. After exiting circulation, leukocytes migrate through tissue interstitial spaces where they generate forces to deform surrounding cells which in turn apply confining pressures to regulate cell morphology and motility[3–6]. Existing *in vitro* migration platforms have uncovered that the degree of mechanical confinement and resulting variations in local cell shape regulate leukocyte speed, directionality, polarity, and migration mode[5,7–12], thus implicating a role of local

mechanical pressures in regulating the immune response. In the absence of confinement, leukocyte migration is largely mediated by actin polymerization-driven formation of a pseudopod at the leading edge[3,4,13,14]. However, under confinement by external pressures, leukocytes can elect for an alternative migration strategy driven by rear acto-myosin contractility driving membrane protrusions (blebs) through rapid fluctuations in internal hydrostatic pressure[3,4,6,12,15,16].

While widely accepted that local pressures applied by surrounding cells regulate immune cell trafficking, characterization of these interactions *in vivo* is currently limited. Furthermore, existing *in vitro* systems to study confined cell migration largely utilize materials orders of magnitude stiffer than cells themselves (**Fig. S1**) and therefore fail to accurately recapitulate physical interactions with surrounding cells. The development of hydrogels with tunable elasticity and pore size has yielded critical insights into how cell-matrix interactions modulate migration speed and directionality[17–22], however neglect to model interactions with surrounding cells (stiffness ~ 200-3000 Pa on single cell length scales[23]). Furthermore, these systems remain highly complex; tunable to only an average pore size or bulk stiffness, and offer limited control over individual fiber stiffness (~300 MPa[5,23]) that migrating cells interact with. To allow for more precise control over both chemical and physical parameters, alternative approaches utilize polymeric materials such as polyacrylamide, agarose, or polydimethylsiloxane (PDMS) based microchannels to study how controlled confinement of individual cells modulates cell traction[24], polarity[25,26], migration direction[27–29], and speed[9,30]. However, the rigidity of these materials restrict modeling pressures exerted by surrounding cells themselves. Thus, there remains an unmet need for engineering an *in vitro* material interface that responds to cell-generated forces to model physical interactions with neighboring cells and enable new insights into how migrating cells sense and respond to local mechanical cues to regulate motility mechanisms.

Here, we first leverage the optical transparency of the zebrafish to characterize physical interactions between neutrophils, the most abundant cell in the immune system, and surrounding cells during interstitial migration. To model these mechanical interactions *in vitro*, we utilize differential surface patterning of a glass substrate to control the spatial geometry of a liquid-liquid (oil-media) interface to construct migration channels on single cell length scales. By examining physical interactions between neutrophils and the interface, we find that the pressures exerted by the interface (governed by interfacial tension) are comparable to those exerted by surrounding cells *in vivo*. The platform is constructed under a layer of oil, allowing for direct physical access to biological samples and thus incorporation of a fibrous collagen coating in channels of sub-10 µm length scales. Cells that reach the interface first (pioneer cells) require greater interfacial deformation than trailing cells and as a result migrate slower. Akin to surrounding cells during interstitial migration, the interface deforms in response to neutrophil-generated forces, resulting in a gradient of confining pressure across single cells. Tuning channel geometry alters confining pressure gradients to recapitulate protrusion morphology and deformations of surrounding cells during migration *in vivo*. We find that neutrophils elect for a bleb-based mechanism of force generation driven by Rho-kinase mediated rear contractility to deform the interface. Altogether, this work introduces a tunable material interface that replicates single cell-scale confining forces within a system accessible to a broad range of researchers to study how cells sense and respond to interactions with the local physical environment to regulate motility.

RESULTS

Characterizing neutrophil mechanical interactions with surrounding cells during interstitial migration in the zebrafish

While widely acknowledged that physical interactions with surrounding cells regulate immune cell trafficking, limitations in optical access have restricted characterization of these interactions *in vivo*. Here, we leverage the genetic tractability and optical transparency of larval zebrafish to characterize interactions between migrating neutrophils and surrounding cells in the skin of a dual-transgenic zebrafish expressing mCherry in neutrophils and GFP in basal keratinocytes (*Tg(mpx:mCherry) x Tg(Krtt1c19e-acGFP))*. The basal keratinocytes form a single layer of cells in the epidermis at three days post-fertilization (dpf) (**Fig. 1a**). Time-lapse imaging of homeostatic migration reveals dynamic variations in neutrophil morphology. (**Fig. 1b**). Imaging of surrounding keratinocytes reveals that shape dynamics are heavily influenced by surrounding cell architectures which mechanically confine migrating neutrophils to dictate morphology (**Fig. 1c**). To counteract these confining pressures, neutrophils exert forces to deform surrounding keratinocytes to create space for migration (**Fig. 1d**). These deformations are quantifiable and elastic in nature (**Fig. 1e**). Taken together, these data establish an *in vivo* model of leukocyte interstitial migration to characterize neutrophil deformations of surrounding cells. Given emerging interest in how local mechanical interactions with surrounding tissues regulate leukocyte trafficking, we sought to construct a tunable *in vitro* platform to model this phenomenon.

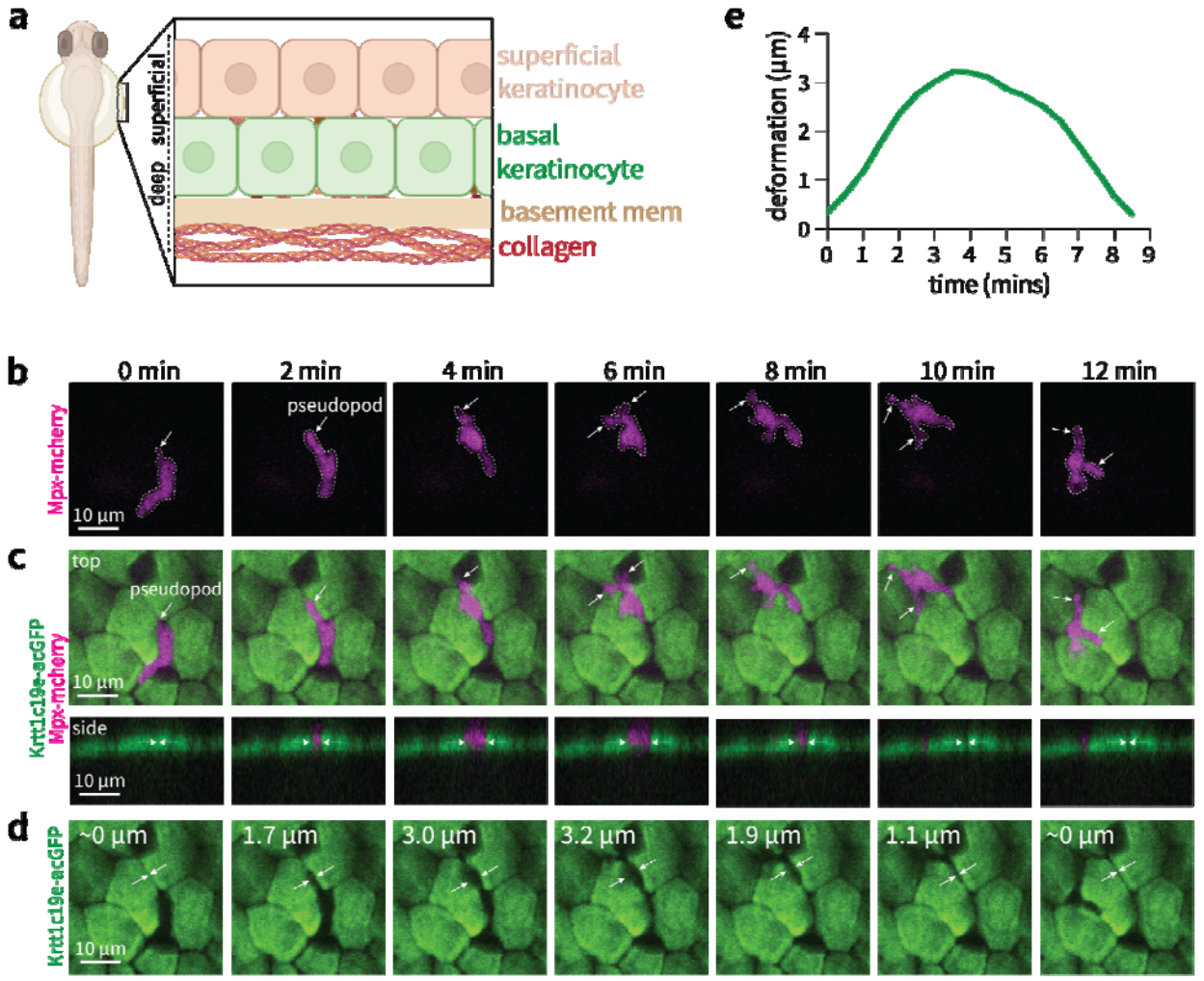

Fig. 1 Neutrophils mechanically interact with and deform surrounding keratinocytes during interstitial migration in zebrafish. a, Schematic of skin layers in zebrafish three days post-fertilization (dpf). **b,** Time-lapse images of migrating neutrophils within the skin **c,** Multi-view visualization of neutrophil interaction with surrounding basal keratinocytes reveals influence of surrounding cell architecture on neutrophil morphology **d,** Resulting deformations of surrounding keratinocytes during neutrophil passage. **e,** Temporal quantification of keratinocyte deformations during neutrophil passage (n = 3 events, taken over 3 independent fish, shaded area represents standard deviation at each time point).

Construction of collagen coated microchannels of a liquid-liquid interface on single-cell length scales

To study how neutrophil interaction with a deformable interface such that of surrounding cells regulates motility, we engineered microfluidic channels composed of culture media confined by a liquid-liquid interface with surrounding oil (oil-media interface). Recently, groups have engineered similar liquid-walled microfluidic channels by either printing aqueous media onto a chemically homogeneous solid substrate under oil overlay[8,31,32], or by depositing media onto superhydrophilic regions of a chemically patterned (i.e., heterogeneous) substrate[33]. In both cases, interfacial forces within the three phase (solid-media-oil) system resist fluid expansion and thus pin the aqueous media to user-controlled geometries. These open systems overcome a number of limitations of traditional PDMS-based microfluidic channels by reducing need for specialized fabrication equipment, decreasing timescales of channel creation from hours to seconds, and allowing for direct physical access to samples through the oil overlay (opposed to a PDMS barrier). However, under aforementioned methods, length scales of purely liquid channels are limited to the millimeter scale. Interrogation of cell interactions with the oil-media interface requires construction of conduits with heights on comparable length scales to single cell diameter (~ 10 µm). Here, we leverage a recent discovery of exclusive liquid repellency (ELR)[34–36] to control interface geometry with the theoretical maximum of liquid-confining forces, enabling engineering of conduit heights comparable to that of single cells (~1-10 µm) (**Fig 1a**). Channels are constructed by chemical patterning of a glass surface to establish regions exclusively repellent to aqueous media (Water Repellent Surface, WRS) or exclusively repellent to oil (Oil Repellent Surface, ORS) (**Fig. 1b**, **Fig. S2**). Because WRS areas completely repel culture media and ORS areas completely repel oil, this double-ELR system provides the theoretical maximum of interfacial forces to pin both media and oil onto their preferred surface[36], enabling the construction of channels with a range of heights (1-10 µm) less than single cell diameter. Media is deposited onto the pre-patterned glass surface by “sweeping” a hanging

droplet of media across the surface with a pipette to construct > 40 channels on a standard microscope slide within seconds (**Fig. 2c**). Here, we implement a pattern that results in two hemispheric droplets with a connecting liquid channel (**Fig. 2d**). Channel geometry is governed by user-controlled pattern selection; a channel of 35 µm width has a height of < 2 µm (**Fig. 2e**).

While collagen is the most abundant extracellular matrix (ECM) protein in the body and provides physical and chemical[37] cues to migrating cells, its high viscosity and rapid polymerization rate limits incorporation into traditional closed microchannels on sub-100 µm length scales. Existing methods often require external pumping of collagen into closed channels[38], decreasing throughput and increasing adoption barrier. Here, channels are constructed in open fluid, allowing for direct physical access so that performing the sweep technique with neutralized collagen yields microchannels on single cell length scales made of fibrillar collagen (**Fig. 2f-g, Fig. S3**).

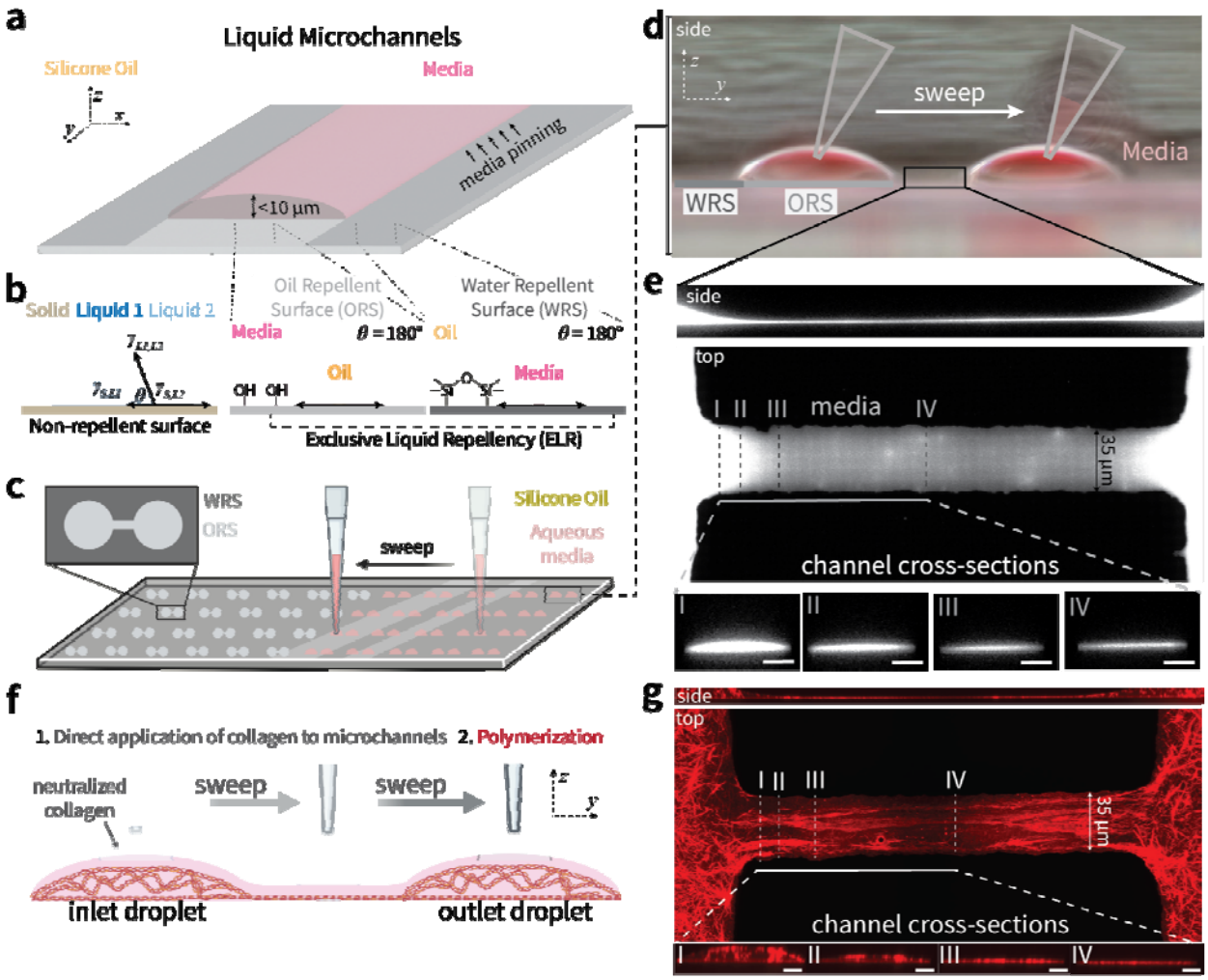

Fig. 2 ELR-enabled construction of collagen-coated liquid microchannels on single cell length scales. a, Schematic of liquid channels with heights comparable to that of single cells (range < 10 µm controlled by channel design). **b,** Schematic representation of differential chemical patterning resulting in a double ELR system (ORS is oil in media ELR and WRS is media in oil ELR). **c,** Schematic of channel construction by "sweeping" aqueous media across ORS regions to form two hemispheric droplets and a connecting channel (> 40 on standard microscope slide). **d,** Macroscale side view of a channel after sweep and addition of 1µL of culture media to each droplet to improve visualization. **e,** Confocal image of 35 µm width culture media channel and < 1 µm height (scale bars represents 10 µm). The channel height tapers at the entrance to a relatively consistent height (points c-d) until a gradual increase towards the

channel exit. **f,** Schematic depicting incorporation of fibrous collagen into microchannels by direct pipetting through the oil layer. **g,** Representative confocal image of 35 µm width collagen-coated channel (scale bars represents 4 µm).

Interfacial tension of liquid-liquid interface exerts cell-scale pressures to confine yet deform in response to the presence of a cell

Existing *in vitro* platforms to study confined migration largely rely on rigid materials that do not generate confining pressures of similar magnitude to single cell-scale forces. Here, we leverage the interfacial pressures enabled by generation of a liquid-liquid interface with controlled curvature to mechanically confine cells. Neutrophils placed directly into channels (**Fig. 3a**) of decreasing size (200 µm to 30 µm channel widths) exhibit decreasing cell height, implicating sufficient force applied by the interface to mechanically confine single cells (**Fig. 3b**, interface denoted by dashed line). However, the presence of cells deforms the channel revealing that the oil-media interface is not a rigid barrier such as plastic or PDMS elastomer (stiffness ~ 300 MPa) but is deformable by the presence of individual cells (**Fig. 3c-d**). This suggests that the interfacial tension of the liquid-liquid interface provides confining pressures comparable to single cell stiffness. The pressure applied by a curved liquid-liquid interface is governed by the LaPlace equation; a function of the interfacial free energy between the liquid phases (γ_{OM} ~ 41.8 mN/m for water and silicone oil[39]) and the radii of interfacial curvature across all curved planes. Within this mathematical framework, interfacial pressure at positions where cells are present (black line) is controllable by varying channel width and thus height (gray line) (**Fig. 3e**). The result is an ability to control the degree of cell confinement as a function of channel geometry (**Fig. 3f**).

As neutrophils mechanically interact with surrounding cells, chemokine gradients arising from sites of injury or infection also influence migration path and speed. The generation of chemokine gradients to study cell migration within *in vitro* systems requires physical separation

of cells from chemical cues, commonly achieved by physically patterning cells in space using rigid walls[40–42]. Given that the liquid-liquid interface exerts pressures sufficient to confine cells, we hypothesized that this interface could act as a physical barrier to allow spatial trapping of cells at the channel entrance. Thus, channels were constructed with collagen, followed by sequential addition of cells to the inlet droplet by direct pipetting (**Fig S4a**). The result is a layer of media upon a layer of fibrillar collagen (**Fig. S4b**). If the oil-media interface possesses sufficient rigidity to spatially trap cells within the media layer, then the media layer height would control cell positioning along the entrance to the channel. We find that cells become spatially trapped at the entrance to the channel where interfacial height is comparable to neutrophil diameter (~ 8-12 μm[43]) (**Fig S4c**). Addition of FITC to the outlet droplet establishes a chemical gradient that is stable over experimental timescales (at least 3 hours) (**Fig S4d-f**). Taken together, these results demonstrate the ability to use a liquid-liquid interfacial barrier to spatially control cell positioning within a chemical gradient within open, physically accessible channels.

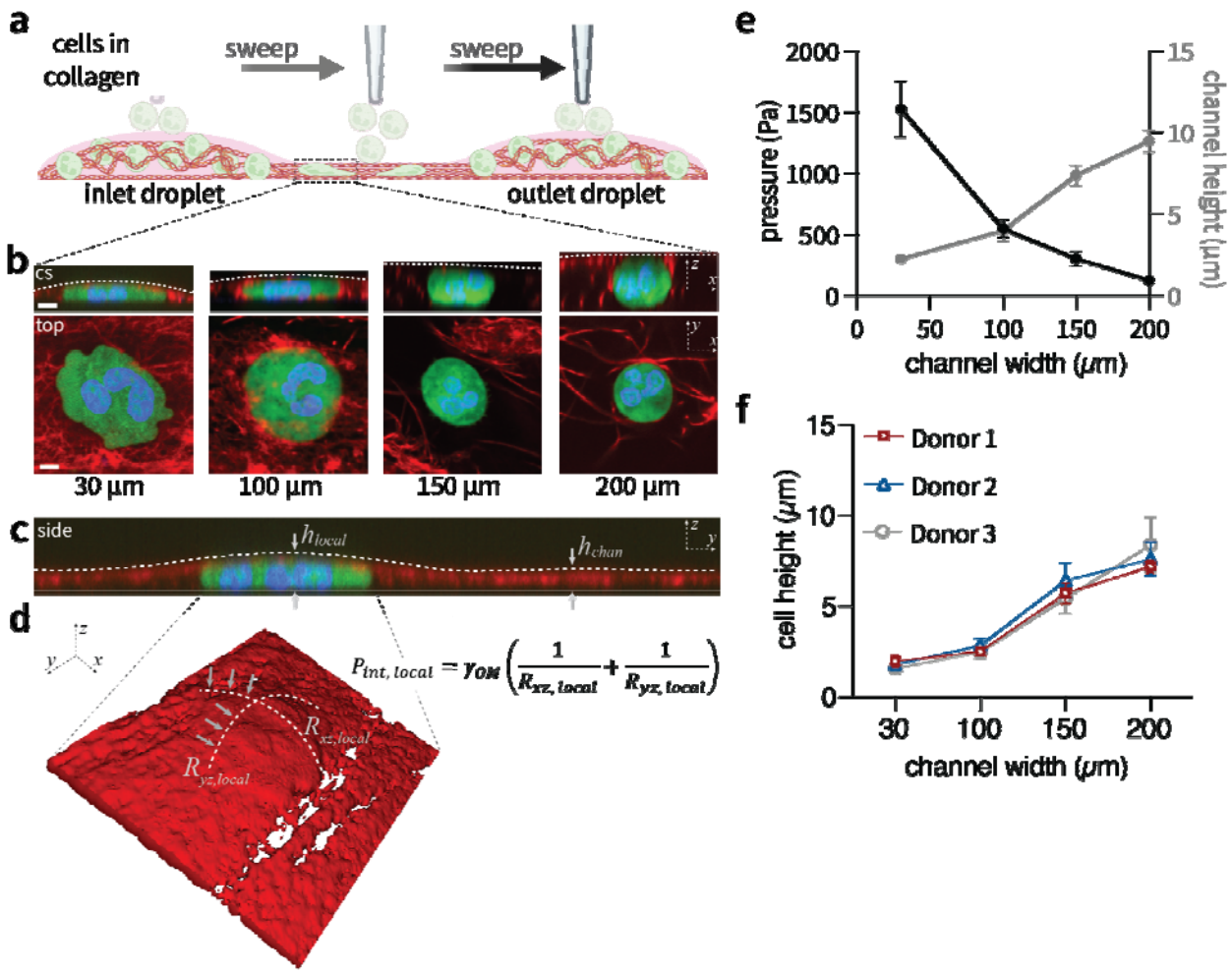

Fig. 3 Mechanical confinement of neutrophils by the interfacial tension of a liquid-liquid interface. a, Schematic depicting direct addition of cells embedded in collagen into liquid microchannels. **b,** Neutrophils placed within channels of varying width (30-200 µm) and thus height exhibit differential degrees of cell confinement. **c,** Channel side view revealing that cells are confined by, yet deform the channel interface to generate curvature in the *zy* plane. **d,** Confocal surface rendering of channel deformation in the *xz* and *zy* planes with confining pressure exerted by the interface modeled by the Young-Laplace equation. **e,** Channel height (gray) and confining pressures (black) as a function of channel width (n = 3 channel replicates). **f,** Degree of confinement, measured by cell height, as a function of varying channel width (n = 3 channel replicates per donor).

Neutrophil migration speed is dependent on required deformation of the interface

Creation of collagen coated channels followed by sequential addition of neutrophils opposite from chemoattractant enables the study of confined neutrophil migration along a collagen substrate (**Fig. 4a**). Cells occupy the layer of culture media between the collagen coating and oil-media interface, thus chemotaxis would require active deformation of the channel interface to allow space for migration (**Fig. 4b**). The initial cells to enter the channel, denoted as “pioneer” cells, migrate slowly, followed by “trailing” cells that migrate rapidly (**Fig. 4c-d**). Confocal imaging reveals differential interface heights before and after pioneer cell passage (**Fig. 4e**), suggesting that pioneer cells actively deform the interface to allow space for migration. Similar to surrounding cells *in vivo*, the interface is elastic, so that it relaxes after leader cell passage (**Fig. S5a-b**). However, on average, trailing cells are subjected to significantly higher channel heights than pioneer cells (**Fig. 4f**). The differential migration speed of pioneer and trailing cells is not explained by alterations in the chemical gradient (**Fig. S5c-d**) or signal relay mechanisms characteristic of neutrophil swarming[44,45] (**Fig. S5e-f**). Rather, these data suggest a model whereby the required deformation of the interface decreases migration speed. To further decouple chemical cues from physical changes in interface height, we analyzed a subset of trailing cells that migrate fast enough to catch up to and thus become pioneer cells. These cells are exposed to the same chemical gradient as pioneer cells (**Fig. S5d**), yet significantly decrease in speed as they reach the interface (**Fig. 4g**). Taken together, these data indicate a mechanical mechanism whereby pioneer cells actively deform the channel interface, leaving a higher interfacial height for trailing cells which in turn require less deformation and migrate faster. Critically, these results demonstrate the ability to decouple chemical cues such as position within a gradient, from mechanical cues of interfacial height, to isolate the role of physical cues on cell motility.

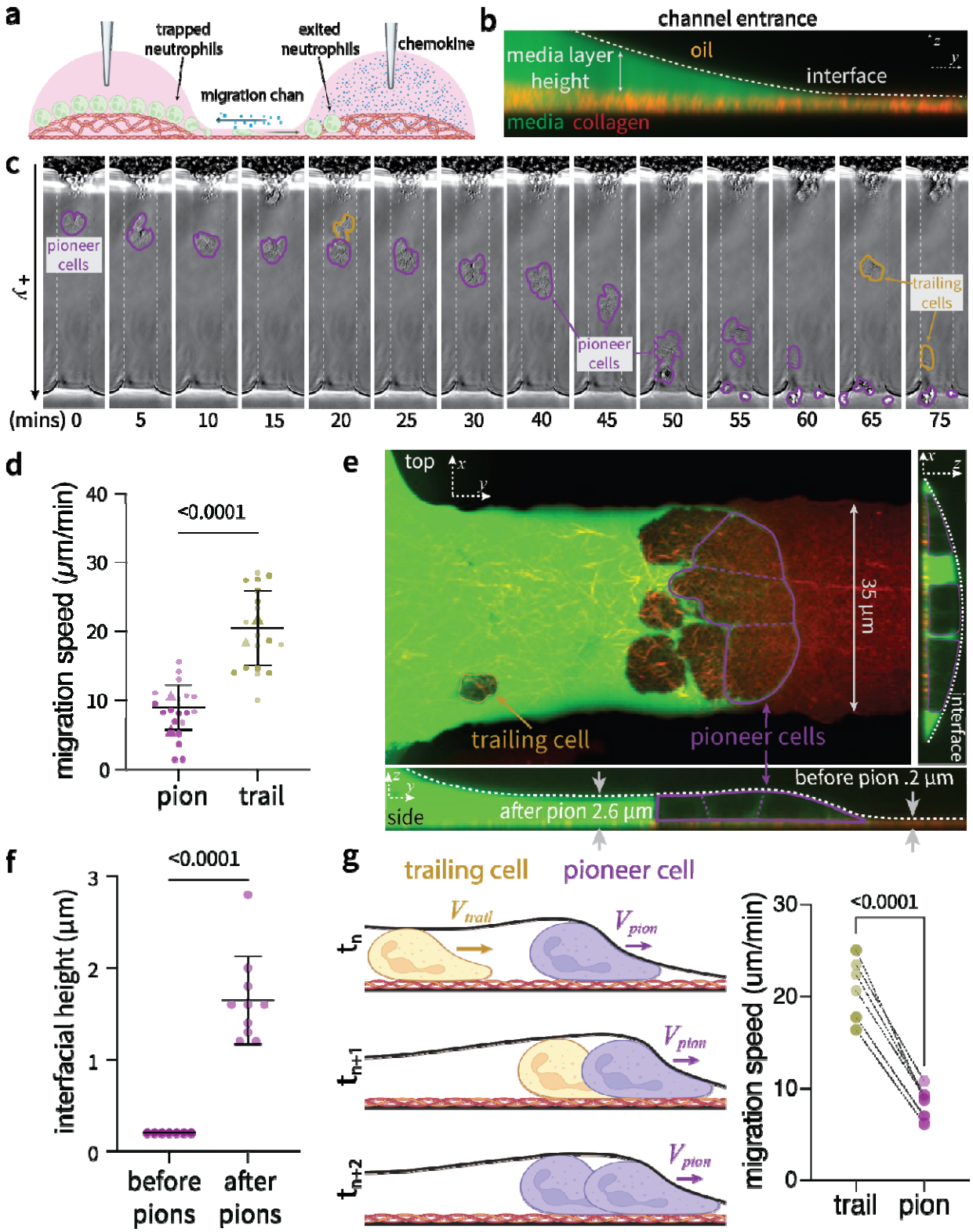
a
trapped neutrophils
exited neutrophils
chemokine
migration chan
b
channel entrance
media layer height
oil
interface
media
collagen
c
pioneer cells
trailing cells
+y
(mins) 0
5
10
15
20
25
30
40
45
50
55
60
65
75
d
migration speed (μm/min)
<0.0001
pion
trail
e
top
35 μm
trailing cell
pioneer cells
interface
side
before pion .2 μm
after pion 2.6 μm
f
interfacial height (μm)
<0.0001
before pions
after pions
g
trailing cell
pioneer cell
V_{trail}
V_{pion}
t_n
t_{n+1}
t_{n+2}
migration speed (um/min)
<0.0001
trail
pion

255

Fig. 4 Migration speed is dependent on required deformation of interface. a, Schematic of migration experiment **b,** Representative (confocal) side view of channel entrance. Cells are confined to the media layer between the collagen coating and oil-media interface. **c,** Timelapse images and **d,** corresponding plots characterizing differential migration speeds of pioneer and trailing cells (n = 5 cells depicted by circles over 3 channel replicates; triangles represent independent donor means) **e,** Confocal imaging of pioneer cells and interfacial geometry **f,** Quantification of interfacial heights before and after passage of pioneer cells. **g,** Model schematic and corresponding migration speed of neutrophils that start as trailing cells but catch up to and become pioneer cells over time. Each data point represents a cell (taken from an independent channel) and shade represents donor.

Tuning interfacial geometry yields a gradient of confining pressure across a single cell to recapitulate deformations of surrounding cells during interstitial migration *in vivo*

During interstitial migration, neutrophils utilize internal machinery to generate forces to deform and migrate between surrounding cells. In response, surrounding cells exert opposing confining pressures. The balance between neutrophil-generated and surrounding cell-generated pressures govern cell shape which regulates motility[5,7,46]. In the zebrafish, we find that neutrophils first extend a protrusion to exert force on surrounding keratinocytes, followed by a period of maximal keratinocyte deformation during passage of the cell body (**Fig. 5a**). Pioneer cells in liquid channels exhibit similar extension of a protrusion to deform the liquid interface, with maximal interfacial deformation occurring during passage of the cell body (**Fig. 5b**). Where cell confinement by traditional agarose or PDMS-based methods generate fixed confining pressures across a cell, the liquid-liquid interface responds to neutrophil-generated pressures resulting in a gradient of confining force over the length of a single pioneer cell. This pressure gradient is tunable by controlling channel geometry (**Fig. 5c-d, Fig. S6a-c**) without significantly affecting the chemokine gradient (**Fig. S6d)**. Controlling confining pressure gradients within a

range of 200-1500 Pa replicates protrusion width (**Fig. 5e**), maximal keratinocyte deformations (**Fig. 5f**), and speed of neutrophil passage (**Fig. 5g**) during interstitial migration *in vivo*. These data demonstrate the ability to model mechanical interactions between leukocytes and surrounding cells *in vivo* within microchannels formed by a liquid-liquid material interface.

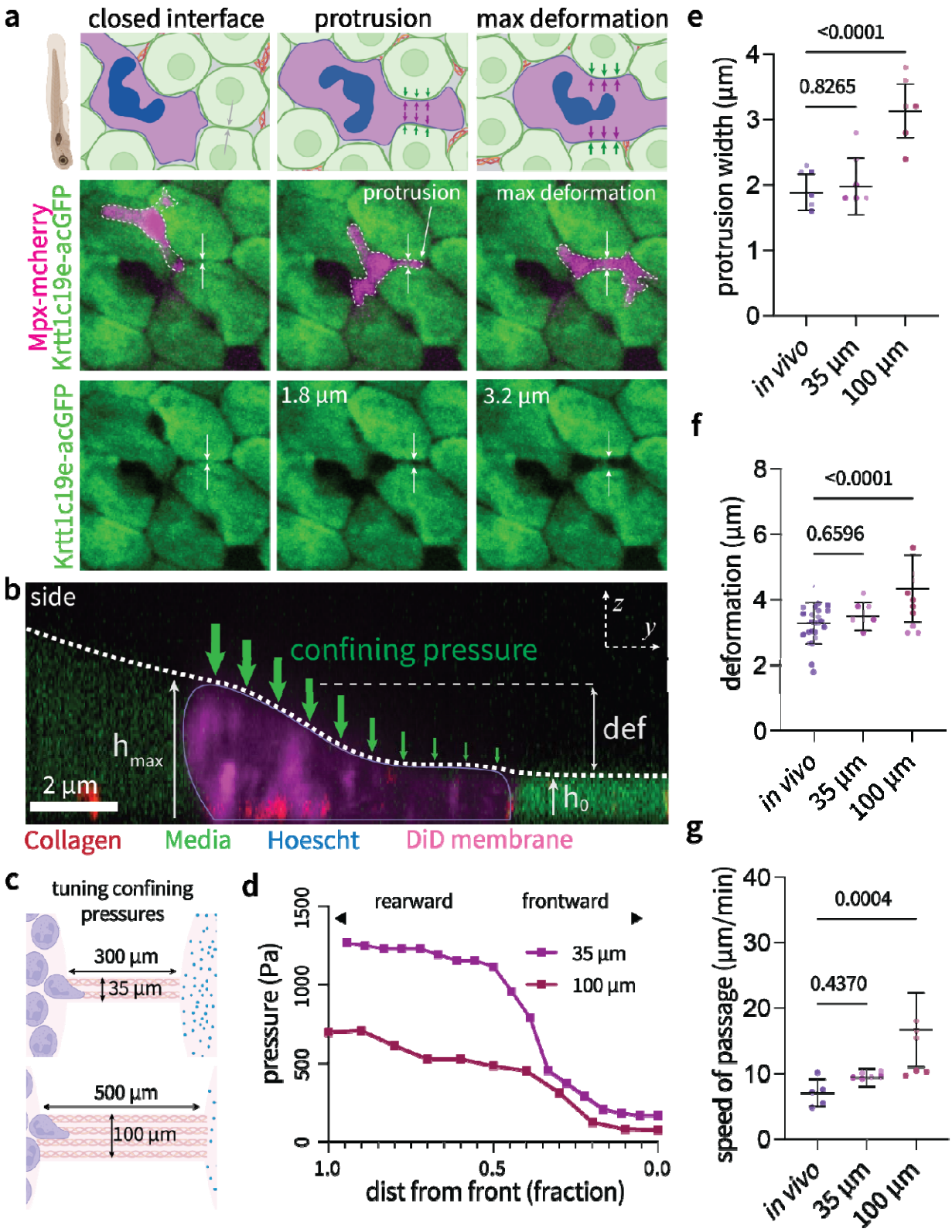
a
closed interface
protrusion
max deformation
Mpx-mcherry
Krtt1c19e-acGFP
protrusion
max deformation
Krtt1c19e-acGFP
1.8 µm
3.2 µm
b
side
confining pressure
z
y
def
h max
2 µm
h0
Collagen
Media
Hoescht
DiD membrane
c
tuning confining pressures
300 µm
35 µm
500 µm
100 µm
d
rearward
frontward
35 µm
100 µm
pressure (Pa)
dist from front (fraction)
e
<0.0001
0.8265
protrusion width (µm)
in vivo
35 µm
100 µm
f
<0.0001
0.6596
deformation (µm)
in vivo
35 µm
100 µm
g
0.0004
0.4370
speed of passage (µm/min)
in vivo
35 µm
100 µm

287

Fig. 5 Tuning confining pressure gradients across a single cell recapitulates neutrophil morphologies during interstitial migration *in vivo*. a, Confocal imaging depicting distinct phases of interstitial migration *in vivo* whereby neutrophils extend a protrusion to deform surrounding keratinocytes followed by passage of the cell body resulting in maximal deformation of surrounding cells. **b,** Representative confocal image of migration in liquid channels. The interface responds to cell generated forces yielding a gradient of confinement across a single cell. **c,** Schematic depicting tunability of channel geometries and thus confining interfacial pressures. **d,** Representative pressure gradients confining pioneer cells within channels that yield differential radii of interfacial curvature. **e-g** Tuning channel confining pressures recapitulates width of neutrophil protrusions, maximal keratinocyte deformations, and speed of passage through surrounding keratinocytes *in vivo*. Circles represent single cell passage events, with shade depicting independent fish or channel replicate. Statistical significance was determined by a one-way ANOVA assuming equal variances with multiple comparisons to the *in vivo* group.

Neutrophils employ a bleb-based mechanism of force generation mediated by Rho-Kinase to deform an interface exerting cell-scale confining pressures

The mechanisms by which leukocytes exert force to deform surrounding cells during interstitial migration is not fully understood. On two-dimensional surfaces, leukocytes largely rely on polymerization of branched actin networks stabilized by actin-related protein 2/3 (Arp2/3) at the leading edge to extend protrusions. Recent studies have demonstrated that under confinement, neutrophils can employ a bleb-based motility mechanism independent of actin polymerization at the leading edge[16] whereby contraction at the rear drives increased hydraulic pressure leading to rapid projections of the cell membrane (blebs) at the leading edge (**Fig. 6a**). Here, we find that migration speed is significantly impaired by treatment with Arp-2/3 inhibitor CK666 in an established two-dimensional migration system (**Fig. S7)**, however is unaffected within liquid

channels (**Fig. 6b**). This suggests a migration mode independent of actin polymerization at the leading edge under confinement within liquid channels. Given that pioneer cells extend protrusions to deform the liquid-liquid interface (**Fig. 5b above**), we investigated the mechanisms of force generation employed by neutrophils at the leading edge. Pioneer cells actively deforming the interface exhibit a greater number of bleb-like protrusions compared to trailing cells (**Fig. 6c-e, Supplemental Movie 2-3**). Furthermore, inhibition of rear contractility under treatment with Rho-Kinase inhibitor Y-27632 hinders the ability of pioneer cells to migrate through the deformable interfacial barrier (**Fig 6f**). Taken together, these data support a mechanism whereby pioneer cells favor a bleb-based mechanism of force generation driven by Rho-Kinase-mediated rear contractility to deform and migrate through an elastic interface exerting cell-scale confining pressures.

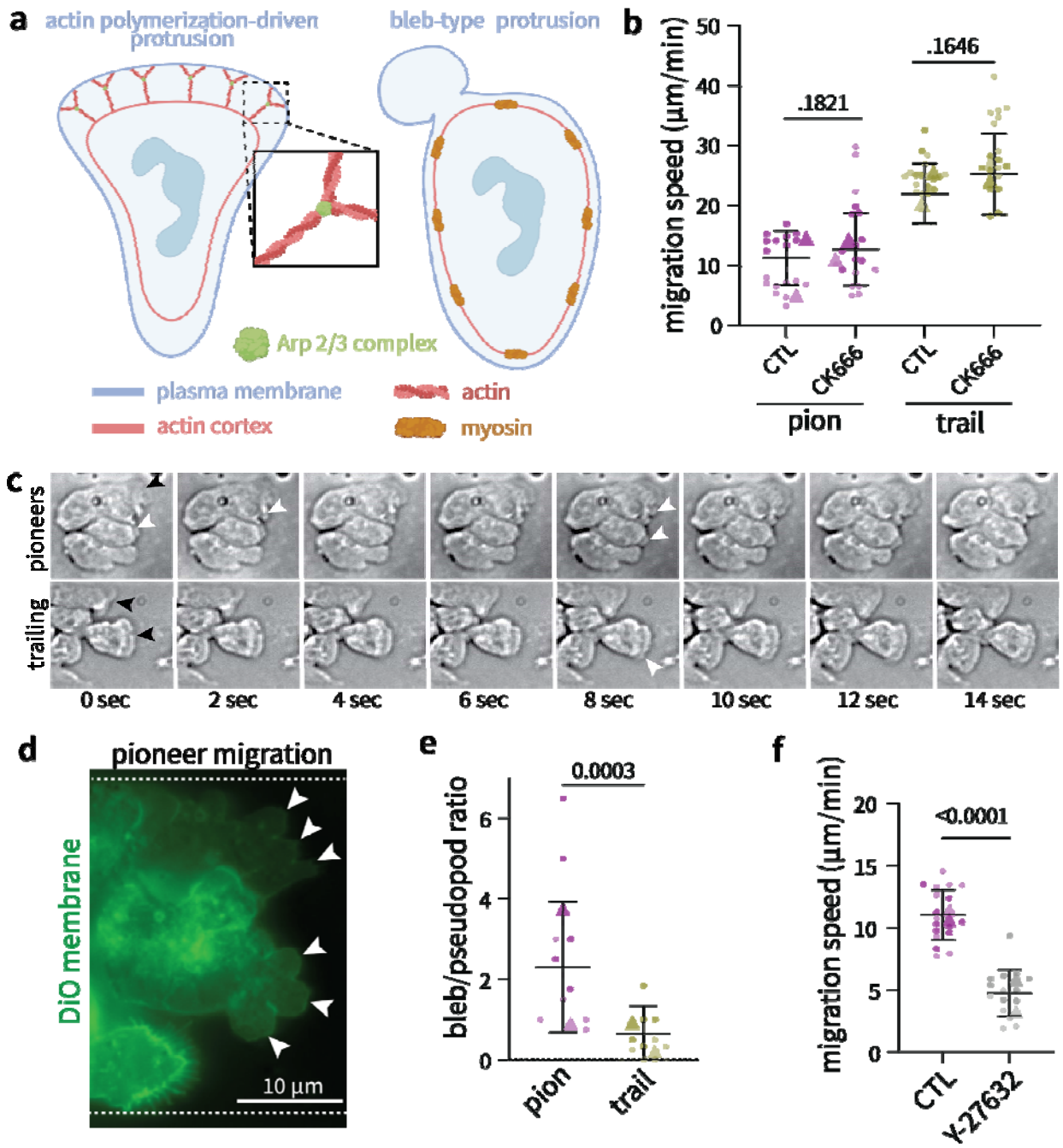

Fig. 6 Neutrophils employ a bleb-based mechanism of force generation to deform confining interface. a, Schematic of leukocyte migration modes, including actin polymerization-dependent pseudopod formation and bleb formation through rear contraction driving membrane extension. **b,** Treatment with Arp2/3 inhibitor CK666 does not impact migration speed within liquid channels. Circles represent individual cells over three independent channels represented

by shade; triangles represent independent donors. **c,** Timelapse images of bleb (white arrows) and pseudopod (black arrows) formation in pioneer and trailing cells. **d,** Pioneer cells exhibit bleb-like protrusions at the leading edge. **e,** Pioneer cells interacting with the interface exhibit a higher bleb to pseudopod ratio than trailing cells. **f,** Inhibition of rear contractility with Rho Kinase inhibitor Y-27632 decreases pioneer migration speed.

DISCUSSION

While largely accepted that physical interactions with surrounding cells regulate immune cell trafficking to sites of tissue injury, infection, or malignancy, challenges in optical access have limited the characterization of these interactions *in vivo*. Where a great deal of literature focuses on immune cell exit from circulation through the endothelial cell layer[47–52], immune cells must traverse long distances through interstitial spaces of host tissue to reach sites of inflammation. Here, we establish an *in vivo* model of neutrophil interstitial migration in an optically transparent, dual transgenic larval zebrafish to characterize physical interactions between neutrophils and surrounding keratinocytes. We then leverage pressures generated by the interfacial tension of a liquid-liquid interface of controlled geometry to model these interactions. By tuning confining pressure gradients across a single cell, physical interactions with the *in vitro* interface recapitulate leukocyte shape dynamics and surrounding tissue deformations characteristic of *in vivo* interstitial migration. Critically, spatial and temporal variations in confining pressures are reflected by instantaneous interfacial curvature. Thus, while existing methods of measuring cell-generated forces largely rely on active experimental intervention (i.e. atomic force microscopy) or mapping onto known substrate characteristics (i.e. traction force microscopy)[53], the use of liquid-liquid interfaces of controlled geometries offers the potential to read out instantaneous force data across a single cell through application of established interfacial physics.

Utilizing this platform, we uncover that interactions with a deformable interface exerting cell-scale confining pressures regulate neutrophil chemotaxis. Pioneer cells that first reach the

channel require greater interfacial deformation to allow space for migration and as a result migrate slower. These results would predict impaired leukocyte recruitment through tissues composed of stiffer cells, or more tightly packed cellular architectures. Given the temporal changes in tissue architecture that occur over various disease states (i.e. tissue wounding, infection, malignancy)[2,52,54,55], understanding how altered tissue mechanics regulates host immune cell motility mechanisms holds particular relevance to human disease. While previous studies have shown that Arp2/3-driven perinuclear actin polymerization is required for dendritic cell passage through PDMS-based microchannel mechanical constrictions[56], parallel studies have shown that Arp2/3 is dispensable for neutrophil migration under mechanical confinement in PDMS-channels, whereby neutrophils adopt a branched-actin independent migration mechanism[16]. Here, we find that branched-actin stabilization is dispensable for neutrophil migration under a confining yet elastic material interface. Furthermore, we uncover for the first time that neutrophils elect for a bleb-based mechanism of force generation to deform an interface that responds to cell-generated pressures. From both a cell biology and engineering perspective, this work advances our understanding of how the external physical environment regulates leukocyte migration strategies while introducing an *in vitro* platform to further investigate how migrating cells integrate chemical and mechanical cues to regulate motility. Further elucidation of how immune cells sense and respond to physiologically relevant physical cues might facilitate development of therapeutic approaches targeting immune cell migration machinery in the context of human disease.

METHODS

Zebrafish maintenance and handling

Animal care and use was approved by the Institutional Animal Care and Use Committee of University of Wisconsin and strictly followed guidelines set by the federal Health Research

Extension Act and the Public Health Service Policy on the Humane Care and Use of Laboratory Animal, administered by the National Institutes of Health Office of Laboratory Animal Welfare. All protocols using zebrafish in this study were approved by the University of Wisconsin-Madison Research Animals Resource Center (protocol M005405-A02). Previously published transgenic lines *Mpx:mCherry*[57] and *Krtt1c19e:acGFP (Gift of Dr. Alvaro Sagasti)* were maintained on the AB background. Following breeding, fertilized embryos were transferred to E3 medium (5 mM NaCl, 0.17 mM KCl, 0.44 mM $CaCl_2$, 0.33 mM $MgSO_4$, 0.025 mM NaOH, and 0.0003% Methylene Blue) and maintained at 29°C. Larval zebrafish were anesthetized using 0.2 mg/ml tricaine (ethyl 3-aminobenzoate; Sigma-Aldrich) before any experimentation or live imaging.

Tracking *in vivo* keratinocyte deformations

Dechorionated, tricaine-anesthetized 3 or 4 days-post fertilization (dpf) larvae were mounted in 2% low-melting point agarose (Sigma-Aldrich) on a 35 mm glass bottom dish (#1.5H Glass, Cellvis, CA, USA). Time-lapse imaging of neutrophil migration through basal keratinocytes in the yolk sac was performed on an spinning-disk confocal (CSU-X; Yokogawa) on a Zeiss Observer Z.1 inverted microscope and an electron-multiplying charge-coupled device Evolve 512 camera (Photometrics), with a EC Plan-Neofluar 40×/NA 0.75 air objective (1-2µm optical sections, 2,355 × 512 resolution) using ZenPro 2012 software (Zeiss).

Construction of liquid-liquid microchannels

A chambered coverglass (no. 1.5 borosilicate glass, 0.13 to 0.17 mm thick; Thermo Fisher Scientific, 155360) was treated first with O2 plasma (Diener Electronic Femto, Plasma Surface Technology) at 60 W for 3 min and then moved to an oven for grafting of PDMS-Silane (1,3-dichlorotetramethylsiloxane; Gelest, SID3372.0) (about 10 µl per device) onto the glass surface by chemical vapor deposition (CVD) for 30 mins. The PDMS-grafted slide was masked by a

PDMS stamp (stamp construction described in *Li et al, Science Advances*[36]) and treated with O_2 plasma at 60 W for 3 min. After surface patterning, the PDMS stamp was removed by tweezers and stored in a clean space for reuse. The chambered coverglass slides were overlaid with oil (silicone oil, 5 cSt; Sigma-Aldrich, 317667) to generate an ELR surface. Liquid-liquid channels are created by sweeping a hanging droplet across the O2-plasma patterned surface by a pipette. Channels can be constructed with collagen by sweeping a 1:1:1 solution of rat tail collagen I (Corning, 10 mg/mL)) neutralized with one part neutrophil culture media (Roswell Park Memorial Institute (RPMI) 1640 Medium, Thermo Fisher Scientific,11875093) + 2% fetal bovine serum (Thermo Fisher Scientific, 10437010)) and one part 2X HEPES buffer, yielding a final concentration 3.33 mg/mL of rat tail collagen and pH 7.2. For experiments requiring visualization of the collagen layer, one in 15 parts RFP-labeled rat tail collagen was added to allow for confocal imaging of fiber architecture. The collagen solution was incubated at 37° Celsius for 15 minutes to allow for polymerization before transfer to an on-stage incubator (Bold Line, Okolab) for imaging.

Whole blood collection and neutrophil isolation

All blood samples were drawn according to Institutional Review Boards (IRB) approved protocols per the Declaration of Helsinki at the University of Wisconsin-Madison in the Beebe Lab (IRB# 2020−1623) and in the Huttenlocher Lab (IRB#, 2017-003). Informed consent was obtained from all subjects in the study. Whole blood was collected with standard ethylenediaminetetraacetic acid (EDTA) tubes (BD, #36643, EDTA [K2] STERILE, 1054688) and then stored at RT (~22 °C) or 37 °C in stationary storage before isolation.

Neutrophils were isolated from whole blood using magnetic bead-based negative selection per protocol using either the EasySep Direct Human Neutrophil Isolation Kit (STEMCELL, 19666) or the MACSxpress Neutrophil Isolation Kit (Miltenyi Biotech, 130-104-434) purified with the MACSxpress Erythrocyte Depletion Kit (Miltenyi Biotech, 130-098-196). After isolation, the neutrophil pellet was directly resuspended in RPMI culture media with 2% FBS (as above). Following resuspension, liquid cultures were stored at 37° in a standard CO2 incubator (Thermo Scientific, HERACELL 240i) for no more than 1 hour before transfer to an onstage incubator for imaging.

Cell migration experiments and interface analysis

Cells in media were added to the inlet droplet of collagen channels at concentration 40k cells/µL and 1 µL of 100 nM of neutrophil chemoattractant *N*-Formylmethionyl-leucyl-phenylalanine (fMLP) added to the outlet droplet. After adding, the cell suspension was mixed by pipetting to ensure homogeneity and cell positioning near the channel entrance. The channels were kept at 37 °C, 21% O2, 5% CO2, and 95% RH in an incubator before transfer to an onstage incubator (Bold Line, Okolab) for time lapse imaging on either an epi-fluorescent microscope (Nikon Eclipse TE3000 with a Nikon Plan Fluor 20x/0.50 objective, motorized stage from Ludl Electronic Products and Prime BSI Express camera from Teledyne Photometrics or a Nikon TI Eclipse inverted microscope with Nikon Plan Fluor 20x/0.50 objective and Hamamatsu camera) or a spinning disk confocal microscope (Zeiss microscope described above or a Nikon A1R inverted Ti2 microscope courtesy of the UW-Madison Optical Core. Confocal images were taken at 40x or 63x with a z-step of 200 nm. In the context of inhibitor experiments, cells were incubated in media containing 400 nM MK866 to inhibit LTB4, 10 µm LY-27632 to inhibit Rho-Kinase, or 10 µm CK666 to inhibit Arp2/3 for 30 minutes before the onset of experimentation. Tracking of cell speed was performed in ImageJ/FIJI using the manual tracking plug-in of time lapse movies taken at time intervals of 30 seconds. Cell blebbing events were captured by

imaging at a time interval of 500 ms. Confining pressures was calculated manually by drawing circles around cells within channels in the cross-sectional (xz plane) and side view (yz plane) to estimate radius of curvature. Measurements were performed on cells directly placed into channels by sweeping the collagen solution with cells suspended at 40k/uL concentration, or on migrating cells initially seeded to the inlet droplet. In each case, cells were labeled with nuclear dye Hoescht 33342 (Invitrogen, H1399) and either membrane dye Vybrant DiD or DiO (Invitrogen, V22887) or cytoplasmic dye Calcein-AM (Invitrogen, C3100MP) per Invitrogen protocols.

Statistical Analysis

Data were analyzed (Prism 9.0; GraphPad Software). Statistical significance was assessed using Student's *t* tests when comparing two conditions/groups, and when comparing more than two groups, significance was assessed using one-way analysis of variance (ANOVA) corrected using the Tukey's test.

ACKNOWLEDGEMENTS

The authors would like to thank the University of Wisconsin Imaging Core for the use of microscopy facilities as well as Biorender and Imaris for use of software to make figure schematics.

DECLARATION OF CONFLICTS OF INTEREST

David J. Beebe holds equity in Bellbrook Labs LLC, Tasso Inc., Salus Discovery LLC, Lynx Biosciences Inc., Stacks to the Future LLC, Flambeau Diagnostics LLC, and Onexio Biosystems LLC.

FUNDING ACKNOWLEDGEMENTS

This work was funded by the following grants:

Carbone Cancer Center Cancer Center Support Grant
University of Wisconsin
NIH P30CA014520

Microscale models of inflammation and its resolution
NIH R01AI34749
PI: Beebe and Huttenlocher

Cell Migration and Wound Repair
NIH R35GM118027-08
PI: Huttenlocher

A multiplexed micro scale assay for real time analysis of pediatric immune cell function
NIH U24AI152177
PI: Beebe

Under-oil open microfluidic system (UOMS) for studying systemic fungal infection
NIH R01AI54940
PI: Beebe

Biotechnology Training Program
University of Wisconsin-Madison
T23GM135066
PI: Brian Fox

AUTHOR CONTRIBUTIONS

JHS, AH, TR, CL, AH, DJB. designed the experiments. CL initiated development of the under-oil cell migration platform with the assistance from MF, JL, and JHS. JHS, AH, MF, KL, JL, CWT, JJS, DB, CL performed the experiments. TY and JHS performed macroscopic imaging of microchannel geometries. JHS and KL analyzed the data. CL, DJB, JHS analyzed the interfacial physics during migration within liquid microchannels. JHS, CL, AH, DJB interpreted the data. JHS, CL, AH, DJB wrote the manuscript. All authors reviewed and approved the manuscript.

REFERENCES

1. Luster, A. D., Alon, R. & von Andrian, U. H. Immune cell migration in inflammation: present and future therapeutic targets. *Nat Immunol* **6**, 1182–1190 (2005).
2. de Oliveira, S., Rosowski, E. E. & Huttenlocher, A. Neutrophil migration in infection and wound repair: going forward in reverse. *Nat Rev Immunol* **16**, 378–391 (2016).
3. Moreau, H. D., Piel, M., Voituriez, R. & Lennon-Duménil, A.-M. Integrating Physical and Molecular Insights on Immune Cell Migration. *Trends in Immunology* **39**, 632–643 (2018).
4. Friedl, P. & Weigelin, B. Interstitial leukocyte migration and immune function. *Nat Immunol* **9**, 960–969 (2008).
5. Heuzé, M. L. *et al.* Migration of dendritic cells: physical principles, molecular mechanisms, and functional implications. *Immunol Rev* **256**, 240–254 (2013).
6. van Helvert, S., Storm, C. & Friedl, P. Mechanoreciprocity in cell migration. *Nat Cell Biol* **20**, 8–20 (2018).
7. Sitarska, E. *et al.* Sensing their plasma membrane curvature allows migrating cells to circumvent obstacles. *Nat Commun* **14**, 5644 (2023).
8. Assaying Macrophage Chemotaxis Using Fluid□Walled Microfluidics - Deroy - 2022 - Advanced Materials Technologies - Wiley Online Library. https://onlinelibrary.wiley.com/doi/full/10.1002/admt.202200279.
9. Boneschansker, L., Yan, J., Wong, E., Briscoe, D. M. & Irimia, D. Microfluidic platform for the quantitative analysis of leukocyte migration signatures. *Nat Commun* **5**, 4787 (2014).
10. Prentice-Mott, H. V. *et al.* Biased migration of confined neutrophil-like cells in asymmetric hydraulic environments. *Proc Natl Acad Sci U S A* **110**, 21006–21011 (2013).
11. Ekpenyong, A. E. *et al.* Mechanical deformation induces depolarization of neutrophils. *Science Advances* **3**, e1602536 (2017).

12. Lämmermann, T. *et al.* Rapid leukocyte migration by integrin-independent flowing and squeezing. *Nature* **453**, 51–55 (2008).

13. Fritz-Laylin, L. K. *et al.* Actin-based protrusions of migrating neutrophils are intrinsically lamellar and facilitate direction changes. *eLife* **6**, e26990.

14. Kienle, K. *et al.* Neutrophils self-limit swarming to contain bacterial growth in vivo. *Science* **372**, eabe7729 (2021).

15. Lämmermann, T. & Germain, R. N. The multiple faces of leukocyte interstitial migration. *Semin Immunopathol* **36**, 227–251 (2014).

16. Graziano, B. R. *et al.* Cell confinement reveals a branched-actin independent circuit for neutrophil polarity. *PLoS Biology* **17**, (2019).

17. Cheng, S.-Y. *et al.* A hydrogel-based microfluidic device for the studies of directed cell migration. *Lab Chip* **7**, 763–769 (2007).

18. François, J. *et al.* The interplay between matrix deformation and the coordination of turning events governs directed neutrophil migration in 3D matrices. *Sci Adv* **7**, eabf3882 (2021).

19. Siemsen, K. *et al.* Tunable 3D Hydrogel Microchannel Networks to Study Confined Mammalian Cell Migration. *Adv Healthc Mater* **10**, e2100625 (2021).

20. Li, X., Sun, Q., Li, Q., Kawazoe, N. & Chen, G. Functional Hydrogels With Tunable Structures and Properties for Tissue Engineering Applications. *Frontiers in Chemistry* **6**, (2018).

21. Ehrbar, M. *et al.* Elucidating the Role of Matrix Stiffness in 3D Cell Migration and Remodeling. *Biophys J* **100**, 284–293 (2011).

22. Reinhart-King, C. A., Dembo, M. & Hammer, D. A. Cell-Cell Mechanical Communication through Compliant Substrates. *Biophysical Journal* **95**, 6044–6051 (2008).

23. Guimarães, C. F., Gasperini, L., Marques, A. P. & Reis, R. L. The stiffness of living tissues and its implications for tissue engineering. *Nature Reviews Materials* **5**, 351–370

(2020).

24. Wang, N., Ostuni, E., Whitesides, G. M. & Ingber, D. E. Micropatterning tractional forces in living cells. *Cell Motil Cytoskeleton* **52**, 97–106 (2002).

25. Wang, F. *et al.* Lipid products of PI(3)Ks maintain persistent cell polarity and directed motility in neutrophils. *Nature Cell Biology* **4**, 513–518 (2002).

26. Tsai, T. Y.-C. *et al.* Efficient Front-Rear Coupling in Neutrophil Chemotaxis by Dynamic Myosin II Localization. *Dev Cell* **49**, 189-205.e6 (2019).

27. Zanotelli, M. R. *et al.* Energetic costs regulated by cell mechanics and confinement are predictive of migration path during decision-making. *Nat Commun* **10**, 4185 (2019).

28. Renkawitz, J. *et al.* Nuclear positioning facilitates amoeboid migration along the path of least resistance. *Nature* **568**, 546–550 (2019).

29. Ambravaneswaran, V., Wong, I. Y., Aranyosi, A. J., Toner, M. & Irimia, D. Directional decisions during neutrophil chemotaxis inside bifurcating channels. *Integr Biol (Camb)* **2**, 639–647 (2010).

30. Hamza, B. *et al.* Retrotaxis of human neutrophils during mechanical confinement inside microfluidic channels. *Integr Biol (Camb)* **6**, 175–183 (2014).

31. Soitu, C. *et al.* Microfluidic chambers using fluid walls for cell biology. *Proceedings of the National Academy of Sciences* **115**, E5926–E5933 (2018).

32. Deroy, C. *et al.* Predicting flows through microfluidic circuits with fluid walls. *Microsyst Nanoeng* **7**, 1–9 (2021).

33. Feng, W. *et al.* Harnessing liquid-in-liquid printing and micropatterned substrates to fabricate 3-dimensional all-liquid fluidic devices. *Nat Commun* **10**, 1095 (2019).

34. Li, C. *et al.* Exclusive Liquid Repellency: An Open Multi-Liquid-Phase Technology for Rare Cell Culture and Single-Cell Processing. *ACS Appl Mater Interfaces* **10**, 17065–17070 (2018).

35. Li, C. *et al.* Double-exclusive liquid repellency (double-ELR): an enabling technology for

rare phenotype analysis. *Lab Chip* **18**, 2710–2719 (2018).

36. Li, C. *et al.* Under oil open-channel microfluidics empowered by exclusive liquid repellency. *Science Advances* **6**, eaay9919 (2020).

37. Zhou, Z., Cui, F., Wen, Q. & Susan Zhou, H. Effect of vimentin on cell migration in collagen-coated microchannels: A mimetic physiological confined environment. *Biomicrofluidics* **15**, 034105 (2021).

38. Burkel, B. *et al.* Preparation of 3D Collagen Gels and Microchannels for the Study of 3D Interactions In Vivo. *J Vis Exp* 53989 (2016) doi:10.3791/53989.

39. Li, C. *et al.* Exclusive Liquid Repellency: An Open Multi-Liquid-Phase Technology for Rare Cell Culture and Single-Cell Processing. *ACS Appl. Mater. Interfaces* **10**, 17065–17070 (2018).

40. Somaweera, H., Ibraguimov, A. & Pappas, D. A review of chemical gradient systems for cell analysis. *Anal Chim Acta* **907**, 7–17 (2016).

41. Wang, X., Liu, Z. & Pang, Y. Concentration gradient generation methods based on microfluidic systems. *RSC Adv.* **7**, 29966–29984 (2017).

42. Abhyankar, V. V., Lokuta, M. A., Huttenlocher, A. & Beebe, D. J. Characterization of a membrane-based gradient generator for use in cell-signaling studies. *Lab Chip* **6**, 389–393 (2006).

43. Liew, P. X. & Kubes, P. The Neutrophil's Role During Health and Disease. *Physiol Rev* **99**, 1223–1248 (2019).

44. Lämmermann, T. *et al.* Neutrophil swarms require LTB4 and integrins at sites of cell death in vivo. *Nature* **498**, 371–375 (2013).

45. Hopke, A. *et al.* Neutrophil swarming delays the growth of clusters of pathogenic fungi. *Nat Commun* **11**, 2031 (2020).

46. Huse, M. Mechanical forces in the immune system. *Nat Rev Immunol* **17**, 679–690 (2017).

47. Schwartz, A. B., Kandasamy, A., Yeh, Y.-T. & Alamo, J. C. del. Neutrophils exhibit distinct migration phenotypes that are modulated by transendothelial migration. *Biophysical Journal* **122**, 269a (2023).

48. Wu, X., A. Newbold, M. & L. Haynes, C. Recapitulation of in vivo -like neutrophil transendothelial migration using a microfluidic platform. *Analyst* **140**, 5055–5064 (2015).

49. Stroka, K. M., Hayenga, H. N. & Aranda-Espinoza, H. Human Neutrophil Cytoskeletal Dynamics and Contractility Actively Contribute to Trans-Endothelial Migration. *PLOS ONE* **8**, e61377 (2013).

50. Rabodzey, A., Alcaide, P., Luscinskas, F. W. & Ladoux, B. Mechanical Forces Induced by the Transendothelial Migration of Human Neutrophils. *Biophysical Journal* **95**, 1428–1438 (2008).

51. Gonzalez, A. L., El-Bjeirami, W., West, J. L., McIntire, L. V. & Smith, C. W. Transendothelial migration enhances integrin-dependent human neutrophil chemokinesis. *Journal of Leukocyte Biology* **81**, 686–695 (2007).

52. Huynh, J. *et al.* Age-Related Intimal Stiffening Enhances Endothelial Permeability and Leukocyte Transmigration. *Sci Transl Med* **3**, 112ra122 (2011).

53. Polacheck, W. J. & Chen, C. S. Measuring cell-generated forces: a guide to the available tools. *Nat Methods* **13**, 415–423 (2016).

54. Plodinec, M. *et al.* The nanomechanical signature of breast cancer. *Nature Nanotech* **7**, 757–765 (2012).

55. Lampi, M. C. & Reinhart-King, C. A. Targeting extracellular matrix stiffness to attenuate disease: From molecular mechanisms to clinical trials. *Science Translational Medicine* **10**, eaao0475 (2018).

56. Thiam, H.-R. *et al.* Perinuclear Arp2/3-driven actin polymerization enables nuclear deformation to facilitate cell migration through complex environments. *Nat Commun* **7**, 10997 (2016).

57. Yoo, S. K. *et al.* Differential regulation of protrusion and polarity by PI3K during neutrophil motility in live zebrafish. *Dev Cell* **18**, 226–236 (2010).